Density Functional Analysis: The Theory of Density-Corrected DFT

Stefan Vuckovic,[†] Suhwan Song,[‡] John Kozlowski,[†] Eunji Sim,*,[‡] and Kieron Burke[†]

[†]Departments of Chemistry and of Physics, University of California, Irvine, California 92697, United States

[‡]Department of Chemistry, Yonsei University, 50 Yonsei-ro Seodaemun-gu, Seoul 03722, Korea

ABSTRACT: Density-corrected density functional theory (DC-DFT) is enjoying substantial success in improving semilocal DFT calculations in a wide variety of chemical problems. This paper provides the formal theoretical framework and assumptions for the analysis of any functional minimization with an approximate functional. We generalize DC-DFT to allow the comparison of any two functionals, not just comparison with the exact functional. We introduce a linear interpolation between any two approximations and use the results to analyze global hybrid density functionals. We define the basins of density space in which this analysis should apply and give quantitative criteria for when DC-DFT should apply. We also discuss the effects of strong correlation on the density-driven error, utilizing the restricted HF Hubbard dimer as an example.
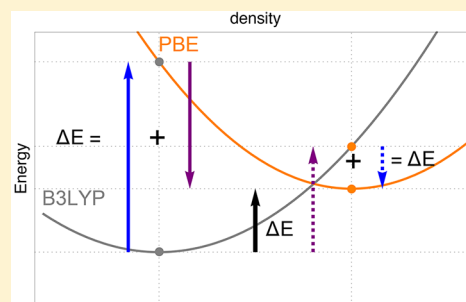
1. INTRODUCTION AND BACKGROUND

Kohn−Sham density functional theory (KS DFT)[1] is widely popular as an electronic structure method.[2] Despite the proliferation of choices of approximate functionals, most calculations use one of a few standard approximations that have been available for the past 20 years, namely, generalized gradient approximations (GGAs) or global hybrids with some enhancements, such as van der Waals corrections[3] and range separation.[4] While moderately accurate for many useful properties, these functionals suffer from well-known deficiencies, including unbound anions, poorly positioned eigenvalues, incorrect molecular dissociation curves, reaction barrier underestimation, and many others,[5,6] thus the never-ending search for improved functionals.

Over the years, many pioneers have shown in specific cases that the use of approximate functionals on Hartree−Fock (HF) densities can yield surprisingly accurate results. This includes the early work of Gordon and Kim for weak forces,[7] Janesko and Scuseria for reaction barriers and other properties,[8,9] and the original works of Gill et al. testing GGAs and hybrids for main group chemistry that led to the adoption of DFT for widespread use in chemistry.[10] Even the prototype of KS-DFT, the X−α method of Slater,[11] was designed to yield approximations to HF potentials, which led to an inconsistency between the associated energy functional and its derivative, the potential. (See ref 12 for a recent discussion of this topic.) An analysis of this difficulty was part of the impetus for the KS paper.

The errors made in DFT calculations were formally separated into two contributions, a functional error and a density-driven error, thereby yielding a formal framework in which the two errors could be analyzed independently.[13] This led to the theory of density-corrected DFT (DC-DFT), which explains the success of the early work, and has provided a simple procedure for significantly improving the results of semilocal DFT calculations in many situations. For example, for halogen and chalcogen weak bonds, which have been used in databases to train van der Waals functionals, the errors are dominated by density-driven errors in the semilocal functional, so such databases cannot be used for that purpose without a correction.[14] In addition to the standard semilocal functionals, it has recently been shown that in specific situations the energetic accuracy of other density functionals, such as the nonlocal functionals based on adiabatic connection models,[15] can be greatly improved by using the HF density and orbitals.[16,17]

Thus, DC-DFT, especially in the form of HF-DFT, in which the Hartree−Fock density is used in place of the exact density, is an extremely practical procedure for improving the energetics of abnormal DFT calculations (i.e., those dominated by density-driven errors, but in which the approximate functional is still highly accurate).

Here, we give a detailed formal analysis of the differences that arise between the self-consistent solutions of two distinct density functionals. We consider any two functionals, including the possibility of two different approximations. Thus, DC-DFT is a special case of this more general analysis. We also consider other special cases, including the one-electron case, for which we can calculate all of the quantities arising from our analysis that require access to the exact functional and the exact density. The accuracy of PBE for the H atom is due to a spurious cancellation of both density and functional errors as well as exchange and correlation errors. We extend our analysis to energy differences that are of key importance in chemistry.

2. DENSITY FUNCTIONAL ANALYSIS

In DFT,[1,2,6,18,19] the ground-state energy and density of a system with an external potential v are given by

$$E_v = \min_n E_v[n] \tag{1}$$

The total energy functional $E_v[n]$ is given by

$$E_v[n] = F[n] + n\cdot v \tag{2}$$

where $n\cdot v = \int d^3r\, n(\mathbf{r})\, v(\mathbf{r})$ and where $F[n]$ is the universal part of the functional commonly partitioned as

$$F[n] = T_S[n] + U_H[n] + E_{XC}[n] \tag{3}$$

$T_S[n]$ is the KS noninteracting kinetic energy functional, $U_H[n]$ is the Hartree energy, and $E_{XC}[n]$ is the exchange-correlation (XC) functional, which in practical calculations must be approximated. Starting from a given approximate or exact XC functional $E_{XC}[n]$, we can write the corresponding approximate universal functional as

$$F[n] = F_{SH}[n] + E_{XC}[n] \tag{4}$$

where $F_{SH}[n]$ is the universal functional within the Hartree approximation, which neglects exchange and correlation effects: $F_{SH}[n] = T_S[n] + U_H[n]$. The minimization in eq 1 is performed over all N-representable densities, and the density that achieves this minimum we denote by n_v. We define an energetic measure of any arbitrary density difference from n_v as

$$D_v[\Delta n] = E_v[n_v + \Delta n] - E_v \geq 0 \tag{5}$$

where eq 1 ensures that $D_v[\Delta n] \geq 0$ for any isoelectronic change in n_v (i.e., $\int d^3r\, \Delta n(\mathbf{r}) = 0$). We refer to this as the energetic distance from the minimum. We can use this measure to say that n is sufficiently close to n_v if

$$D_v[n - n_v] \leq \Delta_c \tag{6}$$

provided that Δ_c is sufficiently small.

Throughout this work, we encounter simple quadratic density functionals, which correspond to normal forms in algebra, and we write

$$A[\Delta n] = \int d^3r' \int d^3r\, A(\mathbf{r}, \mathbf{r}')\, \Delta n(\mathbf{r})\, \Delta n(\mathbf{r}') \tag{7}$$

To gain more insight into the $D_v[\Delta n]$ functional, we can expand $E_v[n]$ around its minimum in a Taylor series[20]

$$E_v[n_v + \Delta n] = E_v + \frac{1}{2}K_v[\Delta n] + O(\Delta n^3) \tag{8}$$

where $\Delta n(\mathbf{r}) = n(\mathbf{r}) - n_v(\mathbf{r})$, and $K_v(\mathbf{r}, \mathbf{r}')$ is given by

$$K_v(\mathbf{r}, \mathbf{r}') = \frac{\delta^2 E_v[n]}{\delta n(\mathbf{r}')\, \delta n(\mathbf{r})}\bigg|_{n=n_v} \tag{9}$$

Combining eqs 2, 4, and 9, we can write $K_v(\mathbf{r}, \mathbf{r}')$ as

$$K_v(\mathbf{r}, \mathbf{r}') = f_{SH}[n_v](\mathbf{r}, \mathbf{r}') + f_{XC}[n_v](\mathbf{r}, \mathbf{r}') \tag{10}$$

where

$$f_{SH}[n](\mathbf{r}, \mathbf{r}') = \underbrace{\frac{\delta^2 T_S[n]}{\delta n(\mathbf{r}')\, \delta n(\mathbf{r})}}_{f_S(\mathbf{r},\mathbf{r}')} + \frac{1}{|\mathbf{r} - \mathbf{r}'|} \tag{11}$$

and

$$f_{XC}[n](\mathbf{r}, \mathbf{r}') = \frac{\delta^2 E_{XC}[n]}{\delta n(\mathbf{r}')\, \delta n(\mathbf{r})} \tag{12}$$

is the static XC kernel. Combining eqs 5 and 8, for an arbitrary and sufficiently small density difference (i.e., $D_v[\Delta n] \leq \Delta_c$), we can write $D_v[\Delta n]$ as

$$D_v[\Delta n] \approx \frac{1}{2}K_v[\Delta n] \tag{13}$$

For any $\Delta n(\mathbf{r})$, satisfying $\int d^3r\, \Delta n(\mathbf{r}) = 0$, we define

$$\Delta n_\beta(\mathbf{r}) = \beta\Delta n(\mathbf{r}) \tag{14}$$

In this way, we can see how far one can go away from $n_v(\mathbf{r})$, in the $\Delta n(\mathbf{r})$ direction, and yet stay within Δ_c energetically. Plugging eq 14 into eq 13, we can easily find the $\beta = \beta_c$ parameter at the boundary (i.e., the one satisfying $D_v[\Delta n_\beta] = \Delta_c$), and it is given by

$$\beta_c = \sqrt{\frac{2\Delta_c}{K_v[\Delta n]}} \tag{15}$$

Note again that we use the notation of eq 7 for the $K_v[\Delta n]$ quantity. The principal goal of the theory outlined here is to carefully analyze the origin of the energy difference that arises between a pair of different density functionals when applied to the same system/process. For a given pair of approximate (or one approximate and the other exact) XC functionals $E_{XC}^{(0)}$ and $E_{XC}^{(1)}$, we define their difference as

$$\Delta E_{XC}[n] = E_{XC}^{(1)}[n] - E_{XC}^{(0)}[n] \tag{16}$$

For a given $v(\mathbf{r})$, the difference in the two ground-state energies arising from a pair of different functionals is

$$\Delta E_v = E_v^{(1)}[n_v^{(1)}] - E_v^{(0)}[n_v^{(0)}] \tag{17}$$

By simply adding and subtracting $E_v^{(1)}[n_v^{(0)}]$ from the r.h.s. of eq 17, we find

$$\Delta E_v = -D_v^{(1)}[-\Delta n_v] + \Delta E_{XC}[n_v^{(0)}] \tag{18}$$

where $\Delta n_v(\mathbf{r}) = n_v^{(1)}(\mathbf{r}) - n_v^{(0)}(\mathbf{r})$. Reversing the choice of 1 and 0, we also find

$$\Delta E_v = \Delta E_{XC}[n_v^{(1)}] + D_v^{(0)}[\Delta n_v] \tag{19}$$

Given that $D_v^{(j)} \geq 0$, eqs 18 and 19 dictate the following chain of inequalities:

$$\Delta E_{XC}[n_v^{(1)}] \leq \Delta E_v \leq \Delta E_{XC}[n_v^{(0)}] \tag{20}$$

By virtue of eq 16, the $\Delta E_{XC}[n_v^{(i)}]$ quantity represents the difference between the two functionals evaluated on each density. Therefore, we can identify $\Delta E_{XC}[n_v^{(1)}]$ and $\Delta E_{XC}[n_v^{(0)}]$ of eqs 18 and 19 as functional-driven terms. On the other hand, $D_v^{(0)}[n_v^{(1)}]$ and $D_v^{(1)}[n_v^{(0)}]$ are the density-driven terms because they are given by the difference between the same energy functional evaluated at different densities. Generalizing the ideas of DC-DFT,[13,14,21−25] for any pair of density functionals, we classify a ΔE_v energy difference as energy- or density-driven. We consider energy-driven ΔE_v as those whose functional-driven terms in eqs 18 and 19 strongly dominate the density-driven terms (i.e., $|\Delta E_{XC}[n_v^{(0)}]| \gg D_v^{(1)}[-\Delta n_v]$ and $|\Delta E_{XC}[n_v^{(1)}]| \gg D_v^{(0)}[\Delta n_v]$). On the other hand, in density-driven cases the density-driven terms are no longer negligible. In Figure 1, we show the two density-driven and the two functional-driven contributions to their energy difference in a
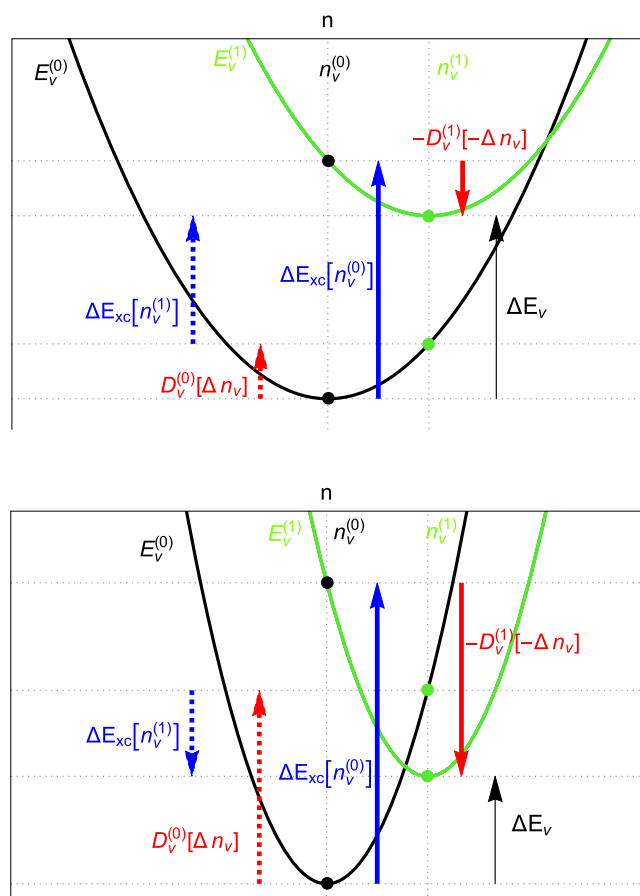
Figure 1. Cartoon showing the density-driven and functional-driven contributions to ΔE_v (eqs 18 and 19) in an energy-driven difference (top panel) and a density-driven difference (bottom panel).

cartoon representing an energy-driven difference (top panel) and a density-driven difference (bottom panel). Measures that quantify density-driven character in a given system (again for a given pair of functionals) will be introduced and discussed in Section 5.

3. DENSITY FUNCTIONAL INTERPOLATION

To derive an exact expression for ΔE_v by smoothly connecting $E_{XC}^{(0)}[n]$ to $E_{XC}^{(1)}[n]$, we introduce the α-parameter-dependent XC functional:

$$E_{XC}^{(\alpha)}[n] = E_{XC}^{(0)}[n] + \alpha \Delta E_{XC}[n] \tag{21}$$

The corresponding total energy functional reads as

$$E_v^{(\alpha)}[n] = \underbrace{F_{SH}[n] + n \cdot v + E_{XC}^{(0)}[n]}_{E_v^{(0)}[n]} + \alpha \Delta E_{XC}[n] \tag{22}$$

and achieves its minimum at $n_v^{(\alpha)}(\mathbf{r})$. Thus, its ground-state energy is given by $E_v^{(\alpha)} = E_v^{(\alpha)}[n_v^{(\alpha)}]$. More generally, we consider the following energy difference:

$$\Delta E_v^{(\alpha)} = E_v^{(\alpha)} - E_v^{(0)} = E_v^{(\alpha)}[n_v^{(\alpha)}] - E_v^{0}[n_v^{(0)}] \tag{23}$$

Writing

$$\Delta E_v^{(\alpha)} = \int_0^\alpha d\alpha' \frac{\partial E_v^{(\alpha')}}{\partial \alpha'} \tag{24}$$

from eq 22, via the Hellmann–Feynman theorem, it follows that

$$\frac{\partial E_v^{(\alpha)}}{\partial \alpha} = \Delta E_{XC}[n_v^{(\alpha)}] \tag{25}$$

Plugging eq 25 into eq 24, we find

$$\Delta E_v^{(\alpha)} = \int_0^\alpha d\alpha' \Delta E_{XC}[n_v^{(\alpha')}] \tag{26}$$

Equation 26 is analogous to, but different from, the adiabatic connection formula for the correlation energy in DFT.[26−28] When $\alpha = 1$, eq 26 becomes

$$\Delta E_v = \int_0^1 d\alpha \, \Delta E_{XC}[n_v^{(\alpha)}] \tag{27}$$

This shows that the energy difference between two KS calculations with different XC functionals can be found by knowing only the difference functional and the interpolating ground-state density. Obtaining ΔE_v from eq 27 requires a knowledge of $n_v^{(\alpha)}(\mathbf{r})$ for all α values between 0 and 1. To find $n_v^{(\alpha)}(\mathbf{r})$, we write the corresponding Euler equation

$$v_{SHXC}^{(0)}[n](\mathbf{r}) + \alpha \Delta v_{XC}[n](\mathbf{r}) + v(\mathbf{r}) \doteq 0 \tag{28}$$

where $v_{SHXC}^{(0)}[n](\mathbf{r}) = \delta F^{(0)}[n]/\delta n(\mathbf{r})$. Because the number of electrons does not change throughout this work, the potentials in eq 28 or any subsequent equations are determined only up to a constant, as denoted by the dot over the equals sign. The density that satisfies eq 28 is $n_v^{(\alpha)}(\mathbf{r})$, and by expanding it around $n_v^{(0)}(\mathbf{r})$ as $n_v^{(\alpha)}(\mathbf{r}) = n_v^{(0)}(\mathbf{r}) + \alpha \Delta n_v^{(\alpha)}(\mathbf{r})$ ($\int d^3r \, n_v^{(\alpha)}(\mathbf{r}) = 0$), we can write eq 28 as

$$v_{SHXC}^{(0)}[n_v^{(0)}](\mathbf{r}) + \alpha[K_v^{(0)} \cdot \Delta n_v^{(\alpha)}](\mathbf{r}) + \alpha(\Delta v_{XC}[n_v^{(0)}](\mathbf{r}) \\ + \alpha[\Delta f_{XC}[n_v^{(0)}] \cdot \Delta n_v^{(\alpha)}](\mathbf{r})) + v(\mathbf{r}) \doteq 0 \tag{29}$$

where we simplified the notation for the following integral:

$$[A \cdot \Delta n](\mathbf{r}) = \int d^3r' \, A(\mathbf{r}, \mathbf{r}') \Delta n(\mathbf{r}') \tag{30}$$

At $\alpha = 0$, eq 28 becomes

$$v_{SHXC}^{(0)}[n_v^{(0)}](\mathbf{r}) + v(\mathbf{r}) \doteq 0 \tag{31}$$

Plugging eq 31 into eq 29 gives

$$[K_v^{(0)}[n_v^{(0)}] \cdot \Delta n_v^{(\alpha)}](\mathbf{r}) + \Delta v_{XC}[n_v^{(0)}](\mathbf{r}) + \alpha[\Delta f_{XC}[n_v^{(0)}] \cdot \Delta n_v^{(\alpha)}](\mathbf{r}) \doteq 0 \tag{32}$$

Also, by plugging $K_v^{(\alpha)}(\mathbf{r}, \mathbf{r}') = K_v^{(0)}(\mathbf{r}, \mathbf{r}') + \alpha \Delta f_{XC}(\mathbf{r}, \mathbf{r}')$ (eqs 10 and 22) into eq 32, we obtain

$$\int d^3r' \, K_v^{(\alpha)}[n_v^{(0)}](\mathbf{r}, \mathbf{r}') \, \Delta n_v^{(\alpha)}(\mathbf{r}') \doteq -\Delta v_{XC}[n_v^{(0)}](\mathbf{r}) \tag{33}$$

In principle, $\Delta n_v^{\alpha}(\mathbf{r}')$ can be obtained by solving eq 33, and we can write the solution in terms of the inverse of $K_v^{(\alpha)}[n_v^{(0)}]$:

$$\Delta n_v^{(\alpha)}(\mathbf{r}) = -\int d^3r' \, \{K_v^{(\alpha)}\}^{-1}[n_v^{(0)}](\mathbf{r}, \mathbf{r}') \Delta v_{XC}[n_v^{(0)}](\mathbf{r}') \tag{34}$$

We expect that $\Delta n_v^{(\alpha)}(\mathbf{r})$ in eq 34 can be fairly approximated by Δn_v, and this is equivalent to approximating $n_v^{(\alpha)}$ via the following linear interpolation:

$$n_v^{(\alpha)}(\mathbf{r}) \approx n_v^{(0)}(\mathbf{r}) + \alpha \Delta n_v(\mathbf{r}) \tag{35}$$

To explore in what situation the approximation of eq 35 becomes exact, we now write $n_v^{(\alpha)}$ as $n_v^{(\alpha)}(\mathbf{r}) = n_v^{(1)}(\mathbf{r}) - \bar{\alpha}\Delta n_v^{(\alpha)'}$, where $\bar{\alpha} = 1 - \alpha$. Repeating the steps given by eqs 28 to 34, we find

$$\Delta n_v^{(\alpha)'}(\mathbf{r}) = -\int d^3 r' \, \{K_v^{(\alpha)}\}^{-1}[n_v^{(1)}](\mathbf{r}, \mathbf{r}')\Delta v_{XC}[n_v^{(1)}](\mathbf{r}') \tag{36}$$

In this way, when $\Delta n_v^{(\alpha)'}(\mathbf{r})$ is equal to $\Delta n(\mathbf{r})$ in eq 34, then the exact $n_v^{(\alpha)}$ is indeed given by the r.h.s of eq 35.

To obtain the leading order of $E_v^{(\alpha)}$ in powers of α, we again set $n_v^\alpha(\mathbf{r}) = n_v^{(0)}(\mathbf{r}) + \alpha\Delta n_v^{(\alpha)}(\mathbf{r})$. Then, $E_v^{(\alpha)}$ becomes

$$E_v^{(\alpha)}[n_v^{(\alpha)}] = F_{SH}[n_v^{(0)} + \alpha\Delta n_v^{(\alpha)}] + n_v^{(0)}\cdot v + \alpha\Delta n_v^{(\alpha)}\cdot v$$
$$+ E_{XC}^{(0)}[n_v^{(0)} + \alpha\Delta n_v^{(\alpha)}] + \alpha\Delta E_{XC}[n_v^{(0)} + \alpha\Delta n_v^{(\alpha)}] \tag{37}$$

We can expand $E_v^{(\alpha)}[n_v^{(0)} + \alpha\Delta n_v^{(\alpha)}]$ around $n_v^{(0)}(\mathbf{r})$ and write $E_v^{(\alpha)}$ in powers of α:

$$E_v^{(\alpha)} = E_v^{(0)}[n_v^{(0)}] + \alpha\Delta E_{XC}[n_v^{(0)}] + \alpha(v_{SHXC}^{(0)}[n_v^{(0)}] + v)\cdot\Delta n_v^{(\alpha)}$$
$$+ \alpha^2\left(\Delta v_{XC}[n_v^{(0)}]\cdot\Delta n_v^{(\alpha)} + \frac{1}{2}K_v^{(0)}[\Delta n_v^{(\alpha)}]\right) + O(\alpha^3) \tag{38}$$

Combining eqs 31 and 38, the third term on the r.h.s of eq 38 vanishes:

$$E_v^{(\alpha)} = E_v^{(0)}[n_v^{(0)}] + \alpha\Delta E_{XC}[n_v^{(0)}] + \alpha^2\left(\frac{1}{2}K_v^{(0)}[\Delta n_v^{(\alpha)}]\right.$$
$$\left. + \Delta v_{XC}[n_v^{(0)}]\cdot\Delta n_v^{(\alpha)}\right) + O(\alpha^3) \tag{39}$$

Using eq 33, we can further simplify eq 39:

$$E_v^{(\alpha)} = E_v^{(0)}[n_v^{(0)}] + \alpha\Delta E_{XC}[n_v^{(0)}] + \frac{\alpha^2}{2}\Delta v_{XC}[n_v^{(0)}]\cdot\Delta n_v^{(\alpha)}$$
$$+ O(\alpha^3) \tag{40}$$

From eq 40, we can see that $E_v^{(\alpha)}$ truncated at second order in α can be obtained from the XC energies and XC potentials at the end points. We can also use the following functional expansion

$$\Delta E_{XC}\left[n_v^{(0)} + \frac{\alpha}{2}\Delta n_v^{(\alpha)}\right] = \Delta E_{XC}[n_v^{(0)}]$$
$$+ \frac{\alpha}{2}\Delta v_{XC}[n_v^{(0)}]\cdot\Delta n_v^{(\alpha)} + O(\alpha^2) \tag{41}$$

and plug it into eq 40 to obtain

$$E_v^{(\alpha)} = E_v^{(0)}[n_v^{(0)}] + \alpha\Delta E_{XC}\left[n_v^{(0)} + \frac{\alpha}{2}\Delta n_v^{(\alpha)}\right] + ... \tag{42}$$

Similarly, writing $n_v^{(\alpha)} = n_v^{(1)}(\mathbf{r}) - \bar{\alpha}\,\Delta n_v^{(\alpha)}(\mathbf{r})$, we can expand $E_v^{(\alpha)}$ around $n_v^{(1)}$ to obtain

$$E_v^{(\alpha)} = E_v^{(1)}[n_v^{(1)}] - \bar{\alpha}\Delta E_{XC}\left[n_v^{(1)} - \frac{\bar{\alpha}}{2}\Delta n_v^{(\alpha)}\right] + ... \tag{43}$$

Both results are consistent with applying eq 26 and expanding only the density to first order in α. In Section 4, we will illustrate the usefulness of the formalism developed in this section for connecting a global hybrid functional to its parent GGA.

4. SPECIFIC CASES

4.1. Quantifying Errors with DC-DFT. There has recently been a great amount of interest in quantifying the errors in density in DFT.[29−33] However, in ref 25, it was shown that the

theory of DC-DFT provides a natural and unambiguous measure of the density error. With that measure, it was not possible to distinguish the densities of empirical and nonempirical functionals based on their self-consistent densities alone.

To understand the background for this, we first must distinguish ground-state KS DFT from other areas of electronic structure. The primary purpose of such calculations is to produce the ground-state energy as a function of nuclear coordinates. Indeed, in principle, one can deduce the density (and hence any integral over it) from a sequence of such calculations via the functional derivative with respect to the potential. Of course, such calculations produce KS potentials, orbitals, and eigenvalues as well as densities and ground-state energies, and all such quantities can be compared (for systems for which the calculation is feasible) to their exact counterparts extracted from a more accurate quantum solver.[34−37] These are of great interest as inputs to response calculations, such as in linear-response TDDFT or GW methods, and such procedures might be extremely sensitive to such inputs. However, in ground-state DFT, the main prediction is the energy of the many-body system, for which the KS scheme is simply a brilliant construct that balances efficiency and accuracy.

Intuitively, one feels that a better XC potential must yield a better density, and in turn, a better density must yield a better energy. After all, the Hohenberg−Kohn (HK) theorem tells us that we reach the ground-state energy only with the exact density and exact KS potential. But such formal statements give no measure of the quality of a density or a potential. Even a well-defined mathematical norm between two densities that vanishes as the exact density is approached does not really provide what we wish for because an infinite number of arbitrarily different norms can be constructed. All can tell us when we have found the exact density but give differing results for how far away we are from it. A deep part of the problem is that both potentials and densities are functions of $\mathbf{r}$ and so are not characterized by a single number.

As mentioned in ref 25, the basic theorems of DFT give us an ideal solution to this dilemma via DC-DFT. To write this measure in the language of the density functional analysis, we consider now the specific case where $E_{XC}^{(0)}[n] = E_{XC}[n]$ is the exact XC functional and where $E_{XC}^{(1)}[n] = \tilde{E}_{XC}[n]$ is an approximate functional. Note also that this is the basis of all DC-DFT applications. For a given $v(\mathbf{r})$, the difference between the two corresponding ground-state energies becomes the error in the approximate ground-state energy:

$$\Delta\tilde{E}_v = \tilde{E}_v - E_v \tag{44}$$

For this special case, eq 19 becomes

$$\Delta\tilde{E}_v = \underbrace{\tilde{E}_v[\tilde{n}_v] - E_v[\tilde{n}_v]}_{\Delta\tilde{E}_{XC}[\tilde{n}_v]} + \underbrace{E_v[\tilde{n}_v] - E_v[n_v]}_{\Delta E^{ideal}[\Delta\tilde{n}_v] = D_v[\Delta\tilde{n}_v]} \tag{45}$$

where $\Delta\tilde{n}_v = \tilde{n}_v - n_v$. For any system, the variational principle (eq 1) ensures that $\Delta E^{ideal}[\Delta\tilde{n}_v]$ is always a positive energy for any $\tilde{n}_v(\mathbf{r})$ and vanishes only for the exact density. Another advantage of $\Delta E^{ideal}[\Delta\tilde{n}_v]$ over other metrics is that this measurement of density error is given in terms of the energetic consequences. A single number, instead of a function that depends on $\mathbf{r}$, determines how good a given approximate density is. As such, it even provides a useful scale for density differences. For example, if this measure yields results in the microhartree range, then why would one even care about

errors in the density? Given that it is very difficult in practice to evaluate the exact functional on an approximate density (e.g., refs 38 and 39), DC-DFT procedures use the following equation instead:

$$\Delta \tilde{E}_v = \underbrace{\tilde{E}_v[\tilde{n}_v] - \tilde{E}_v[n_v]}_{\Delta E_D = -\tilde{D}_v[-\Delta\tilde{n}_v]} + \underbrace{\Delta\tilde{E}_{XC}[n_v]}_{\Delta E_F} \tag{46}$$

Equation 46 allows us to decompose $\Delta\tilde{E}_v$, the total error made by $\tilde{E}_{XC}[n]$ and $\tilde{n}_v$, into the functional error $\Delta E_F = \Delta\tilde{E}_{XC}[n_v]$ and the density-driven error $\Delta E_D = -\tilde{D}_v[-\Delta\tilde{n}_v]$, which is much more practical than the ideal because it needs to be evaluated only on the approximate functional. We can in fact expect ΔE_D to be a practical proxy for the intractable $E^{ideal}[\Delta\tilde{n}_v]$ measure. When the approximate density is sufficiently close to its exact counterpart (more precisely, when the two inequalities hold: $D_v[\Delta\tilde{n}_v] \leq \Delta_c$ and $\tilde{D}_v[-\Delta\tilde{n}_v] \leq \Delta_c$), we can write $\Delta E^{ideal}[\Delta\tilde{n}_v]$ as

$$\Delta E^{ideal}[\Delta\tilde{n}_v] \approx \frac{1}{2}K_v[\Delta\tilde{n}_v] \tag{47}$$

and $\tilde{D}_v[-\Delta n_v]$ as

$$\tilde{D}_v[-\Delta\tilde{n}_v] \approx \frac{1}{2}\tilde{K}_v[\Delta\tilde{n}_v] \tag{48}$$

From eqs 47 and 48, we can see that if the approximate functional has accurate curvature, then the $\tilde{D}_v[-\Delta\tilde{n}_v] = -\Delta E_D$ measure is very similar to $\Delta E^{ideal}[\Delta\tilde{n}_v]$.

4.2. Illustration. Figure 2 illustrates many aspects of the analysis described so far. Here we consider the hydrogen atom
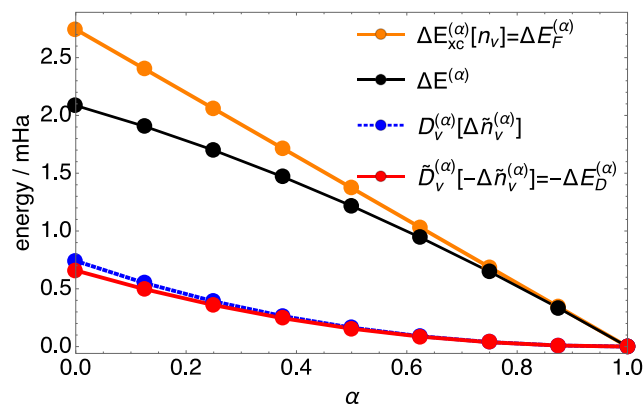

Figure 2. Various errors in eqs 51 and 52 for the α-BLYP calculations of the hydrogen atom as a function of the amount of exact exchange mixing.

and the BLYP GGA.[40,41] We choose this example carefully because (a) we have easy access to the exact density because this is a one-electron case and (b) our functional correctly has no correlation energy (because the LYP correlation vanishes for all fully spin-polarized systems). Thus, when we interpolate between BLYP and HF, we create a global hybrid with a fraction α of exact exchange (EXX):

$$\tilde{E}_{XC}^{(\alpha)}[n] = \tilde{E}_{XC}^{GGA}[n] + \alpha(E_X[n] - \tilde{E}_X^{GGA}[n]) \tag{49}$$

For this specific case, $\tilde{E}_{XC}^{\alpha}[n]$ reduces to

$$\tilde{E}_{XC}^{(\alpha)}[n] = \tilde{E}_X^{B88}[n] + \alpha(E_X[n] - \tilde{E}_X^{B88}[n]) \tag{50}$$

where $E_X^{B88}[n]$ stands for the exchange functional of Becke.[40] For the $\Delta\tilde{E}_v^{(\alpha)} = \tilde{E}_v^{(\alpha)} - E_v$ energy difference (i.e., the error in the hybrids functional), we can rewrite eq 46 as

$$\Delta\tilde{E}_v^{(\alpha)} = \underbrace{-\tilde{D}_v^{(\alpha)}[-\Delta\tilde{n}_v^{(\alpha)}]}_{\Delta E_D^{(\alpha)}} + \underbrace{\Delta\tilde{E}_{XC}^{(\alpha)}[n_v]}_{\Delta E_F^{(\alpha)}} \tag{51}$$

where $\Delta\tilde{n}_v^{(\alpha)} = \tilde{n}_v^{(\alpha)} - n_v$. In eq 51, we can recognize α-dependent density-driven and functional errors. In the same manner, we can rewrite eq 45:

$$\Delta\tilde{E}_v^{(\alpha)} = \Delta\tilde{E}_{XC}^{(\alpha)}[\tilde{n}_v^{(\alpha)}] + D_v[\Delta\tilde{n}_v^{(\alpha)}] \tag{52}$$

In this case, all error contributions (eqs 51 and 52), as shown in Figure 2, vanish at $\alpha = 1$. On the extreme left ($\alpha = 0$), we see that the functional error exceeds the self-consistent error and the density-driven error is negative, as it should be. (Note that $-\Delta E_D$ is plotted in Figure 2.) The functional error is exactly linear, going to zero as $\alpha \to 1$. Notice that the density-driven error must always behave parabolically around $\alpha = 1$.

We also compare the two choices of reference for D_v (blue and red), finding that they are almost identical. This is telling us that the BLYP density is so close to the exact density that the expansion to second order is fine. Moreover, note that as $\alpha \to 1$, the blue and red data points merge and both are on top of a perfect parabola whose curvature is given by $K_v[\Delta n]$ (again as $\alpha \to 1$). Because the self-consistent error is the sum of the functional and density-driven errors, we can deduce its curve just from the values at $\alpha = 0$. Thus, the black line is always a parabola if the densities are sufficiently similar, as is the case here. Note that we can see that the energetic difference between the D_v values (blue and red plots) is rather small, showing that they are indeed sufficiently close that there are no significant energetic consequences to approximating all such curves as parabolas.

Finally, we note that, relative to DC-DFT, we have chosen the two functionals in reverse order: 0 denotes the approximate functional, and 1 denotes the exact answer. This was done to make these results more readily comparable to other results for hybrids. Simply replace α with $1 - \alpha$ to put Figure 2 in the correct form for DC-DFT.

4.3. Self-Interaction Error and One-Electron Systems. For one-electron systems

$$F[n] = T_S[n], \quad E_X[n] = -U_H[n], \quad E_C = 0 \ (N = 1) \tag{53}$$

Standard DFT approximations typically do not satisfy all of the conditions of eq 53, and for this reason, they suffer from one-electron self-interaction error (SIE).[6,42] On the other hand, the HF method is exact for one-electron systems, and thus we can use the HF method to calculate the functional- and density-driven term of SIE. This has already been done in Figure 2 for the BLYP hybrids, and in Figure 3, we apply the same analysis to hybrids from the PBE functional.[43] The PBE correlation energy, unlike that of LYP, does not vanish for one-electron systems. For this reason, in the case of the PBE functional we modify eq 49:

$$\tilde{E}_{XC}^{(\alpha)}[n] = \tilde{E}_{XC}^{PBE}[n] + \alpha(E_X[n] - \tilde{E}_{XC}^{PBE}[n]) \tag{54}$$

In this way, we ensure that the error in the PBE hybrid of eq 54 (hereinafter α-PBExc) vanishes at $\alpha = 1$. Note that this does *not* include PBE0[44] because this PBExc has only 0.75 PBE correlation at $\alpha = 1/4$. In Figure 3, we show the density-driven and functional error in α-PBExc for the hydrogen atom. First,
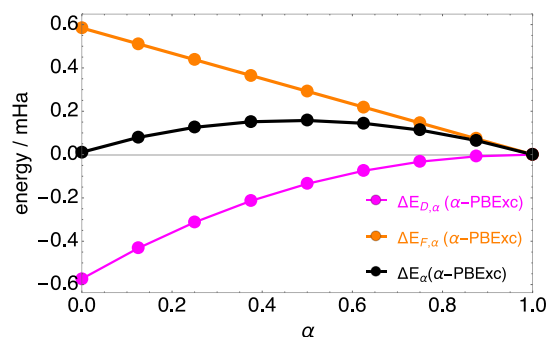
Figure 3. Density-driven and functional errors for the α-PBExc (eq 54) calculations of the hydrogen atom as a function of the amount of exact exchange mixing.

note that the scale of the errors is smaller than that in Figure 2. We can also see that both the $|\Delta E_F^{(\alpha)}|$ and $|\Delta E_D^{(\alpha)}|$ errors in α-PBExc decrease with α. Nonetheless, its total $\Delta E^{(\alpha)}$ error peaks at $\alpha \approx 0.5$ and nearly vanishes for the PBE functional (the $\alpha = 0$ case). The fact that the PBE gives almost the exact energy for the hydrogen atom relies on a cancellation between the functional and density-driven errors (as well as a cancellation between exchange and correlation errors).

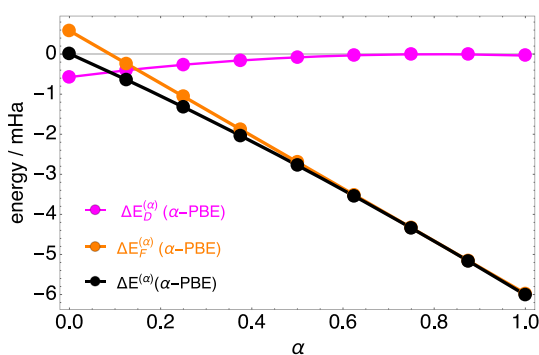The same plot for the hydrogen atom obtained with the regular α-PBE hybrid (eq 49) is shown in Figure 4. Note that

Figure 4. Density-driven and functional errors for the α-PBE (eq 49) calculations of the hydrogen atom as a function of the amount of exact exchange mixing.

now the $\alpha = 1/4$ point represents the PBE0 functional. We can see from Figure 4 that as α approaches 1, the functional error strongly dominates its density-driven counterpart. Note here the much larger scale: the self-interaction error in the PBE correlation functional error yields much larger total energy errors than in the previous figure, illustrating the increased error when semilocal correlation functionals are combined with exact exchange. We can also note that ΔE_D gets very close to 0 as α approaches 1, although the PBE correlation potential does not vanish for $N = 1$ systems.

4.4. Hartree Approximation. Another special case is the Hartree approximation (i.e., solution of the KS equations with XC set to zero). In the Hartree approximation, the functional error is just the XC energy itself, while the density-driven error is just $\Delta E_D = -1/2 f_{SH}[n_v^{(0)}, \Delta n]$. To give an illustration, here we consider again the hydrogen atom and the following functional: $\tilde{E}_{XC}^{(\alpha)}[n] = \alpha E_X[n]$. The $\tilde{E}_{XC}^{(\alpha)}[n]$ functional allows us to analyze the errors along the path that connects the Hartree approximation ($\alpha = 0$) and the exact functional ($\alpha = 1$) for the hydrogen atom. In Figure 5, we show the errors in this
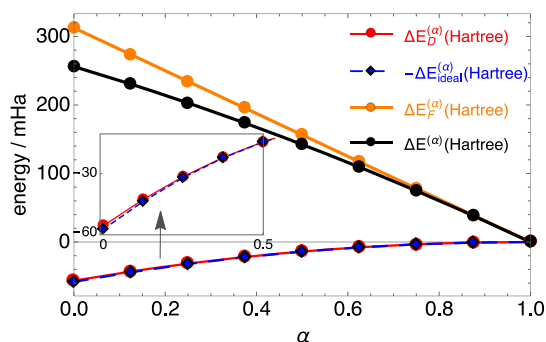

Figure 5. Density-driven, ideal, and functional errors for the hydrogen atom calculation with the $\tilde{E}_{XC}^{\alpha}[n] = \alpha E_X[n]$ functional.

functional as a function of α for the hydrogen atom. As expected, the scale of errors is much larger than those shown in Figures 2−4. For the Hartree approximation, one would expect E_D to be different from the ideal, which includes the XC contributions. However, we can see that the $-\Delta E^{\text{ideal}}$ data points in Figure 5 are hardly distinguishable from their ΔE_D counterparts. This implies that at $\alpha = 0$ (the Hartree approximation) we have

$$\underbrace{f_S[n_v, \Delta n]}_{-2\Delta E^{\text{ideal}}} \approx \underbrace{f_{SH}[n_v^{(0)}, \Delta n]}_{-2\Delta E_D} \text{ (H atom)}$$

$$(55)$$

where $f_S(\mathbf{r}, \mathbf{r}')$ is the kinetic component of $f_{SH}(\mathbf{r}, \mathbf{r}')$ (eq 11).

While Hartree calculations are certainly too inaccurate for chemical purposes,[45,46] one would expect them to have the greatest delocalization error of any approximate functional because not even LDA exchange opposes the Hartree energy. A Hartree calculation might thus prove useful in creating a nonempirical measure of delocalization to be used in DC-DFT because surely no sensible XC approximation should produce a larger density-driven error.

4.5. Pure Density Functionals. So far, we have considered only approximations to XC within the KS scheme because this is the most common DFT calculation today by far. However, there is much interest in developing orbital-free functionals, especially in contexts in which the KS scheme becomes too cumbersome.

Because the entire functional $F[n]$ is approximated in such a scheme, the density is often much poorer than in a KS calculation. In fact, estimates suggest that simple orbital-free approximations, such as those used in Thomas−Fermi theory,[47−49] produce sufficiently poor densities that their errors are dominated by errors in the density (i.e., the density-driven error is much larger than the functional error in most calculations). This is seen in total energy calculations of atoms and of one-dimensional Fermions in a flat box.[23] The simplest DC-DFT in orbital-free DFT is to apply the approximation to the exact density to eliminate the density-driven error.

To exemplify the error analysis of orbital-free functionals, we consider here the TF energy functional, whose universal part reads as

$$F^{TF}[n] = \underbrace{T_S^{TF}[n]}_{A^{TF} \int d^3r\, n(\mathbf{r})^{5/3}} + U[n]$$

$$(56)$$

with $A^{TF} = \frac{3}{10}(3\pi^2)^{2/3}$. The total TF error can be, analogously to eq 46, partitioned as

$$\Delta E_\nu^{\text{TF}} = \underbrace{E_\nu^{\text{TF}}[n_\nu^{\text{TF}}] - E_\nu^{\text{TF}}[n_\nu]}_{\Delta E_D^{\text{TF}}} + \underbrace{\Delta F^{\text{TF}}[n_\nu]}_{\Delta E_F^{\text{TF}}} \tag{57}$$

where $\Delta F^{\text{TF}}[n] = \Delta E_\nu^{\text{TF}}[n] = \Delta T_S^{\text{TF}}[n] - E_{\text{XC}}[n]$. Here we calculate ΔE_D^{TF} and ΔE_F^{TF} for alkaline earth metals and noble gases up to krypton ($Z = 36$). They are computed by utilizing the following for neutral atoms: $E_Z^{\text{TF}} \approx -0.7687 Z^{7/3}$.[50] Highly accurate energies and densities (i.e., E_ν and n_ν entering eq 57) have been obtained with PySCF software[51] at the CCSD level within the aug-cc-pVmZ basis set,[52] with the largest m available for each of the atoms. From the plots shown in Figure 6, we
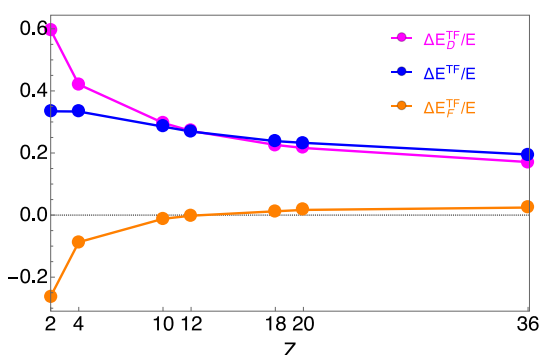

Figure 6. Plots showing quantities that involve the density-driven and functional errors in the Thomas−Fermi method (eq 57) with Z for a range of small atoms.

can see that the density-driven component strongly dominates the total ΔE^{TF} error. For example, in the case of the neon atom ($Z = 10$) most of the TF error is practically density-driven, with $\Delta E_D^{\text{TF}}/E \approx 28.4\%$ and $\Delta E_F^{\text{TF}}/E$ being -1.3%. We remember that for neutral atoms, as $Z \to \infty$, the TF theory becomes relatively exact in the sense that it satisfies[53−55]

$$\lim_{Z \to \infty} \frac{\Delta E_Z^{\text{TF}}}{E_Z} \to 0 \tag{58}$$

Thus, as $Z \to \infty$, our blue curve in Figure 6 should vanish. Nevertheless, in Figure 6 we are still far from this limit, as at our largest Z value ($Z = 36$) $\Delta E_Z^{\text{TF}}/E_Z$ is around 1/5.

This suggests several important points regarding these functionals. First, they must always be tested self-consistently, as in refs 56−58. This is because tests of new orbital-free approximations on KS densities do not tell us much about their overall accuracy, given that the density-driven errors can be very large. At the same time, a comparison of the functional on the KS density then provides enough information to separate functional- from density-driven errors, and we expect that even the KS densities obtained from the (semi)local XC approximations are sufficiently accurate for this purpose. Second, reports of failures of TF theory and its extensions should be revisited to determine if these are density- or functional-driven. If the former, one should focus on improving the densities rather than the total energies alone. Third, this supports efforts[59] to approximate the Pauli potential[60,61] directly as a density functional, without requiring that the KS potential be a functional derivative.

In the context of this article, it should prove useful when comparing two orbital-free approximations to decompose their differences into functional- and density-driven contributions. If two different approximations differ in both contributions, then

this would suggest that good aspects of both might be combined to separately minimize each error.

4.6. Strong Correlation. In our last example, we show that density-driven errors can become large when systems are strongly correlated but need not be. Generating a simple example is not very easy because one needs essentially exact densities upon which to make evaluations and comparisons. Fortunately, the two-site two-Fermion Hubbard model is an example in which all quantities can be determined analytically. Many relevant KS-DFT quantities have been calculated exactly and summarized in two recent reviews: one on the ground state[62] and one on linear-response TDDFT.[63]

For any spin-unpolarized two-electron system (in the absence of magnetic fields), the restricted HF functional (RHF) is

$$F^{\text{RHF}}[n] = T_s[n] + U_H[n]/2 \tag{59}$$

because half the Hartree is canceled by exchange and correlation is ignored. In fact, the traditional definition of correlation energy in quantum chemistry is

$$E_C^{\text{QC}} = E_\nu - E_\nu^{\text{RHF}}[n^{\text{RHF}}] \tag{60}$$

In the RHF case, we have $\tilde{E}_{\text{XC}}[n] = E_X[n]$, and thus

$$\Delta \tilde{E}_{xc}[n] = E_X[n] - E_{\text{XC}}[n] = -E_C[n] \tag{61}$$

From eqs 46 and 61, we obtain the functional error of RHF:

$$\Delta E_F = -E_C[n_\nu] = -E_C \tag{62}$$

By subtracting ΔE_F from the total error made by RHF, which is equal to $-E_C^{\text{QC}}$ (eq 60), we obtain

$$\Delta E_D = E_C - E_C^{\text{QC}} \tag{63}$$

For our two-site model, the functional reduces to a simple function. The onsite occupations are n_1 and n_2 (i.e., the density is just two non-negative real numbers). Moreover, because they always sum to 2, the density is fully represented by their difference. Likewise, we can choose the average potential to be zero and represent the inhomogeneity in the potential by a single number, $\Delta\nu$, the on-site potential difference. If we choose the hopping parameter $t = 1/2$, then the only other parameter is U, the energy cost of double occupation of a site.

The error in RHF and the exact ground-state energy are explored in Figure 7 for varying levels of correlation and inhomogeneity. The absolute error increases with U, as expected. The error in energy for each level of correlation is most prominent in the symmetric dimer ($\Delta\nu = 0$) and diminishes and rapidly vanishes beyond $\Delta\nu$ larger than U,
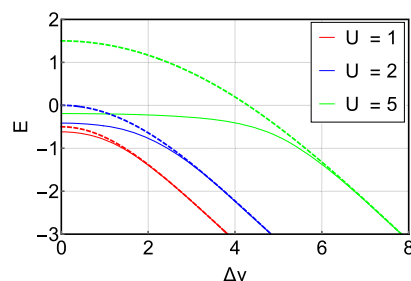

Figure 7. Restricted Hartree−Fock Hubbard dimer ground-state energy (dashed line) and exact Hubbard dimer ground-state energy (solid line) as functions of $\Delta\nu$ for varying values of U. (See ref 62.)

where the energy becomes linearly correlated with the on-site potential difference. Thus, the system becomes weakly correlated for $\Delta v > U$.

The functional- and density-driven contributions to this HF error were then isolated through the use of eqs 60, 62, and 63. The fraction of the total error attributed to the density-driven component $(\Delta E_D / E_C^{QC})$ is shown in Figure 8 for weakly
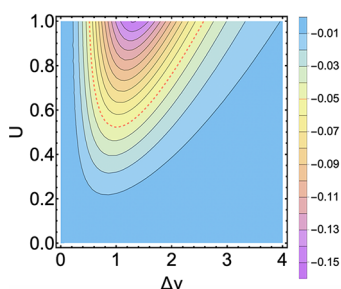

Figure 8. Fraction of the error that is density-driven for moderate values of U, with the 5% contribution contour marked by a red dashed line.

correlated dimers with values of U of up to 1. As U decreases in size, both the magnitude of the total error and its density-driven contribution decrease substantially. For $U < 0.5$, there is no Δv for which there is a density-driven contribution greater than 5% of the total error. Of course, as $U \to 0$, this ratio must vanish, so this is not unexpected. However, we also see that the density-driven error vanishes at $\Delta v = 0$ for any value of U, no matter how large, for symmetry reasons. Thus, even a strongly correlated system might have no density-driven error. Moreover, for $\Delta v > 1 + 2U$, again the error is less than 5% as a result of the correlation being weakened by inhomogeneity. So for any given U, there is a maximum in the fraction of density-driven error as a function of Δv, and it is at nonzero Δv.

The density-driven error ratio for more strongly correlated dimers is shown in Figure 9 and has characteristics identical to
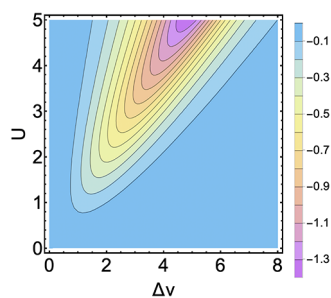

Figure 9. The same as Figure 8 but from more distant perspectives in U and Δv. Note the change in the contour/color scale.

those of the weak correlation plot but on a larger scale. Clearly the maximum fractional density-driven error becomes much larger with U and can even exceed -1. We also see that for $U > 1$ the region of the small density-driven error around $\Delta v = 0$ can even increase with U. For fixed Δv, the fraction of the density-driven error decreases with sufficiently large U. The relation between the RHF density-driven error and strong correlation is clearly not trivial.

To avoid confusion, we note that this section has focused on the density-driven error in RHF. In the more realistic calculations of weakly correlated systems in the rest of this

work, we often assume that the error is much smaller than the density-driven error of a semilocal DFT calculation, and hence HF-DFT yields more accurate energies in such cases. Because the Hubbard dimer is a site model, there is no genuine correspondence with semilocal DFT approximations to test here.

5. ENERGY DIFFERENCES

Key chemical concepts are determined by energy differences (e.g., atomization energies, ionization energies, barrier heights, reaction energies, etc.). So far we have focused on total energies, and in this section we extend our analysis to energy differences. If, for example, we use an approximate functional to calculate an energy difference, what is the density-driven error that pertains to that energy difference? The following analysis answers this question.

For simplicity, we first look at the energy difference between systems A and B, whose external potentials are v_A and v_B, respectively. This energy difference obtained from a total energy functional that corresponds to a given $E_{XC}^{(j)}$ is given by

$$E_{AB}^{(j)} = E_A^{(j)}[n_A^{(j)}] - E_B^{(j)}[n_B^{(j)}] \tag{64}$$

When two functionals are involved, we can also define the difference between $E_{AB}^{(1)}$ and $E_{AB}^{(0)}$:

$$\Delta E_{AB} = E_{AB}^{(1)} - E_{AB}^{(0)} \tag{65}$$

Plugging eq 64 into eq 65 gives

$$\Delta E_{AB} = E_A^{(1)}[n_A^{(1)}] - E_A^{(0)}[n_A^{(0)}] - (E_B^{(1)}[n_B^{(1)}] - E_B^{(0)}[n_B^{(0)}]) \tag{66}$$

Plugging eq 18 into eq 66, we can obtain the counterpart of eq 18 for the energy differences between systems A and B:

$$\Delta E_{AB} = \Delta E_{XC}[n_A^{(0)}] - \Delta E_{XC}[n_B^{(0)}] \underbrace{- D_A^{(1)}[-\Delta n_A] + D_B^{(1)}[-\Delta n_B]}_{-D_{AB}^{(1)}} \tag{67}$$

Similarly, we can also plug eq 19 into eq 66 to obtain the counterpart of eq 19 for the energy differences between systems A and B:

$$\Delta E_{AB} = \Delta E_{XC}[n_A^{(0)}] - \Delta E_{XC}[n_B^{(0)}] + \underbrace{D_A^{(0)}[\Delta n_A] - D_B^{(0)}[\Delta n_B]}_{D_{AB}^{(0)}} \tag{68}$$

In eqs 67 and 68, we recognize $D_{AB}^{(1)}$ and $D_{AB}^{(0)}$ as the density-driven terms pertinent to the energy differences between systems A and B. While $D_v^{(j)}$ of eq 5, which corresponds to the total energies, is always greater or equal to 0, its counterpart that pertains to the energy differences (eqs 67 and 68) does not have a definite sign. Furthermore, if we look at $D_{AB}^{(0)} = D_A^{(0)}[\Delta n_A] - D_B^{(0)}[\Delta n_B]$ (eq 68), where $D_A^{(0)}[\Delta n_A] \geq 0$ and $D_B^{(0)}[\Delta n_B] \geq 0$, we can see that $D_{AB}^{(0)}$ can easily vanish when $D_A^{(0)}[n_A^{(1)}] \approx D_B^{(0)}[n_B^{(1)}]$. Therefore, $D_{AB}^{(0)}$ and $D_{AB}^{(1)}$ can vanish even when $n_A^{(1)}$ and $n_B^{(1)}$ are drastically different from $n_A^{(0)}$ and $n_B^{(0)}$, respectively.

The example that involves the energy difference between systems A and B can be easily generalized to any energy difference of interest. For instance, consider the following chemical reaction

$$\sum_{l=1}^{L} R_l \to \sum_{m=1}^{M} P_m \tag{69}$$

where $\{R_l\}$ is a set of reactants and $\{P_m\}$ is a set of products. Then the energy of this reaction obtained from the $E_v^{(j)}[n]$ functional is

$$E_{\mathrm{ED}}^{(j)} = \sum_{m=1}^{M} E_{\mathrm{P},m}^{(j)}[n_{\mathrm{P},m}^{(j)}] - \sum_{l=1}^{L} E_{\mathrm{R},l}^{(j)}[n_{\mathrm{R},l}^{(j)}] \tag{70}$$

The corresponding difference in $E_{\mathrm{ED}}^{(j)}$ between the $j = 0$ and 1 functionals is

$$\Delta E_{\mathrm{ED}} = E_{\mathrm{ED}}^{(1)} - E_{\mathrm{ED}}^{(0)} \tag{71}$$

Then $D_{\mathrm{ED}}^{(0)}$ that corresponds to ΔE_{ED} is given by

$$D_{\mathrm{ED}}^{(0)} = \sum_{m=1}^{M} D_{\mathrm{P},m}^{(0)}[\Delta n_{\mathrm{P},m}] - \sum_{l=1}^{L} D_{\mathrm{R},l}^{(0)}[\Delta n_{\mathrm{R},l}] \tag{72}$$

and its $D_{\mathrm{ED}}^{(1)}$ counterpart is given by

$$D_{\mathrm{ED}}^{(1)} = \sum_{m=1}^{M} D_{\mathrm{P},m}^{(1)}[-\Delta n_{\mathrm{P},m}] - \sum_{l=1}^{L} D_{\mathrm{R},l}^{(1)}[-\Delta n_{\mathrm{R},l}] \tag{73}$$

In this section we have shown that once we know the density-driven terms that pertain to total energies it is easy to calculate the terms that pertain to energy differences. If we are again interested in the energy difference between systems A and B obtained with an approximate functional, first we can use eq 46 to obtain ΔE_D of that functional pertaining to the total energies of systems A and B. Then, following eqs 67 and 68, we can easily calculate ΔE_D that pertains to the desired energy difference. It will be $\Delta E_D = \Delta E_D[A] - \Delta E_D[B]$. The same analysis can be extended to differentials, such as those determining equilibrium bond lengths or transition-state structures.

6. CONCLUSIONS

We have given a detailed account of the considerations that led to the recent successes of density-corrected DFT. We have also generalized the theory to allow different approximate functionals to be compared in the same way that DC-DFT allows one approximation to be compared with exact results. We have shown that typical density differences between reasonably accurate functionals can be shown quantitatively to be close enough to allow treatment via density functional analysis expansions truncated at second order. We consider different special cases of our analysis and note that DC-DFT is just one of these. For a given pair of density functional approximations, we also discuss their relative abnormality (i.e., the situation in which the density-driven terms strongly dominate the energy difference obtained with two different approximations).

We have noted many pioneering efforts in the chemistry literature in which density-corrected calculations were performed, usually on the basis of intuition. We also point out that, as long ago as 1996, Levy and Görling advocated the use of self-consistent exact-exchange calculations, with a correction defined to produce the exact ground-state energy as a functional of the "wrong" EXX density.[64] For purposes of calculating energies, the approach of Levy and Görling is nearly equivalent to HF-DFT, given that the EXX and HF densities are probably indistinguishable. Of course, we advocate this procedure only for abnormal systems because in normal systems we expect the density from the standard semilocal approximations to be more accurate than that of HF.

Finally, we note that of course it is highly unsettling to run KS calculations in this non-self-consistent fashion. Many advantages that are often taken for granted, such as the exactness of the Hellmann−Feynman theorem in the basis-set limit, are no longer true, and many corrections need to be coded. However, all information about the density can be extracted from a sequence of total energy calculations because

$$n(\mathbf{r}) = \frac{\delta E_v}{\delta v(\mathbf{r})} \tag{74}$$

Treating HF as EXX, this leads to a predicted change in the density of a HF-DFT calculation relative to a self-consistent DFT density:

$$\Delta n(\mathbf{r}) = \frac{\delta(E^{\mathrm{DFT}}[n^{\mathrm{HF}}] - E^{\mathrm{DFT}}[n^{\mathrm{DFT}}])}{\delta v(\mathbf{r})} \tag{75}$$

Thus, in principle, one could calculate the improvement to the density predicted by HF-DFT and any other properties depending only on the density.

■ AUTHOR INFORMATION

Corresponding Author
*E-mail: esim@yonsei.ac.kr.

ORCID ⦿
Stefan Vuckovic: 0000-0002-0768-9176
Suhwan Song: 0000-0002-7768-6181
Eunji Sim: 0000-0002-4139-0960

Notes
The authors declare no competing financial interest.

■ REFERENCES

(1) Kohn, W.; Sham, L. J. Self-consistent equations including exchange and correlation effects. *Phys. Rev.* **1965**, *140*, A1133.
(2) Pribram-Jones, A.; Gross, D. A.; Burke, K. Dft: A theory full of holes? *Annu. Rev. Phys. Chem.* **2015**, *66*, 283−304.
(3) Grimme, S.; Antony, J.; Ehrlich, S.; Krieg, H. A consistent and accurate ab initio parametrization of density functional dispersion correction (DFT-D) for the 94 elements H-Pu. *J. Chem. Phys.* **2010**, *132*, 154104.
(4) Savin, A. In *Recent Developments of Modern Density Functional Theory*; Seminario, J. M., Ed.; Elsevier: Amsterdam, 1996; pp 327−357.
(5) Cohen, A. J.; Mori-Sanchez, P.; Yang, W. Insights into current limitations of density functional theory. *Science* **2008**, *321*, 792.
(6) Cohen, A. J.; Mori-Sánchez, P.; Yang, W. Challenges for density functional theory. *Chem. Rev.* **2012**, *112*, 289.
(7) Gordon, R. G.; Kim, Y. S. Theory for the forces between closed-shell atoms and molecules. *J. Chem. Phys.* **1972**, *56*, 3122−3133.
(8) Scuseria, G. E. Comparison of coupled-cluster results with a hybrid of Hartree−Fock and density functional theory. *J. Chem. Phys.* **1992**, *97*, 7528−7530.
(9) Janesko, B. G.; Scuseria, G. E. Hartree−Fock orbitals significantly improve the reaction barrier heights predicted by semilocal density functionals. *J. Chem. Phys.* **2008**, *128*, 244112.

(10) Gill, P. M.; Johnson, B. G.; Pople, J. A.; Frisch, M. J. The performance of the Becke—Lee—Yang—Parr (B—LYP) density functional theory with various basis sets. *Chem. Phys. Lett.* **1992**, *197*, 499−505.

(11) Slater, J. C. A simplification of the Hartree—Fock method. *Phys. Rev.* **1951**, *81*, 385.

(12) Gritsenko, O.; Mentel, Ł; Baerends, E. On the errors of local density (LDA) and generalized gradient (GGA) approximations to the Kohn-Sham potential and orbital energies. *J. Chem. Phys.* **2016**, *144*, 204114.

(13) Kim, M.-C.; Sim, E.; Burke, K. Understanding and reducing errors in density functional calculations. *Phys. Rev. Lett.* **2013**, *111*, 073003.

(14) Kim, Y.; Song, S.; Sim, E.; Burke, K. Halogen and chalcogen binding dominated by density-driven errors. *J. Phys. Chem. Lett.* **2019**, *10*, 295−301.

(15) Vuckovic, S.; Irons, T. J. P.; Wagner, L. O.; Teale, A. M.; Gori-Giorgi, P. Interpolated energy densities, correlation indicators and lower bounds from approximations to the strong coupling limit of DFT. *Phys. Chem. Chem. Phys.* **2017**, *19*, 6169−6183.

(16) Fabiano, E.; Gori-Giorgi, P.; Seidl, M.; Della Sala, F. Interaction-Strength Interpolation Method for Main-Group Chemistry: Benchmarking, Limitations, and Perspectives. *J. Chem. Theory Comput.* **2016**, *12*, 4885−4896.

(17) Vuckovic, S.; Gori-Giorgi, P.; Della Sala, F.; Fabiano, E. Restoring size consistency of approximate functionals constructed from the adiabatic connection. *J. Phys. Chem. Lett.* **2018**, *9*, 3137.

(18) Burke, K. Perspective on density functional theory. *J. Chem. Phys.* **2012**, *136*, 150901.

(19) Becke, A. D. Perspective: Fifty years of density-functional theory in chemical physics. *J. Chem. Phys.* **2014**, *140*, 18A301.

(20) Ernzerhof, M. Taylor-series expansion of density functionals. *Phys. Rev. A: At., Mol., Opt. Phys.* **1994**, *50*, 4593.

(21) Kim, M.-C.; Sim, E.; Burke, K. Ions in solution: Density corrected density functional theory (DC-DFT). *J. Chem. Phys.* **2014**, *140*, 18A528.

(22) Kim, M.-C.; Park, H.; Son, S.; Sim, E.; Burke, K. Improved DFT potential energy surfaces via improved densities. *J. Phys. Chem. Lett.* **2015**, *6*, 3802−3807.

(23) Wasserman, A.; Nafziger, J.; Jiang, K.; Kim, M.-C.; Sim, E.; Burke, K. The Importance of being Inconsistent. *Annu. Rev. Phys. Chem.* **2017**, *68*, 555−581.

(24) Song, S.; Kim, M.-C.; Sim, E.; Benali, A.; Heinonen, O.; Burke, K. Benchmarks and Reliable DFT Results for Spin Gaps of Small Ligand Fe(II) Complexes. *J. Chem. Theory Comput.* **2018**, *14*, 2304−2311.

(25) Sim, E.; Song, S.; Burke, K. Quantifying density errors in DFT. *J. Phys. Chem. Lett.* **2018**, *9*, 6385−6392.

(26) Harris, J.; Jones, R. The surface energy of a bounded electron gas. *J. Phys. F: Met. Phys.* **1974**, *4*, 1170.

(27) Langreth, D. C.; Perdew, J. P. The exchange-correlation energy of a metallic surface. *Solid State Commun.* **1975**, *17*, 1425−1429.

(28) Gunnarsson, O.; Lundqvist, B. I. Exchange and correlation in atoms, molecules, and solids by the spin-density-functional formalism. *Phys. Rev. B* **1976**, *13*, 4274.

(29) Medvedev, M. G.; Bushmarinov, I. S.; Sun, J.; Perdew, J. P.; Lyssenko, K. A. Density functional theory is straying from the path toward the exact functional. *Science* **2017**, *355*, 49−52.

(30) Kepp, K. P. Comment on "Density functional theory is straying from the path toward the exact functional. *Science* **2017**, *356*, 496−496.

(31) Gould, T. What makes a density functional approximation good? Insights from the left Fukui function. *J. Chem. Theory Comput.* **2017**, *13*, 2373−2377.

(32) Hammes-Schiffer, S. A conundrum for density functional theory. *Science* **2017**, *355*, 28−29.

(33) Korth, M. Density Functional Theory: Not Quite the Right Answer for the Right Reason Yet. *Angew. Chem., Int. Ed.* **2017**, *56*, 5396−5398.

(34) Umrigar, C. J.; Gonze, X. Accurate exchange-correlation potentials and total-energy components for the helium isoelectronic series. *Phys. Rev. A: At., Mol., Opt. Phys.* **1994**, *50*, 3827−3837.

(35) Zhao, Q.; Morrison, R. C.; Parr, R. G. From electron densities to Kohn-Sham kinetic energies, orbital energies, exchange-correlation potentials, and exchange-correlation energies. *Phys. Rev. A: At., Mol., Opt. Phys.* **1994**, *50*, 2138−2142.

(36) Gould, T.; Toulouse, J. Kohn-Sham potentials in exact density-functional theory at noninteger electron numbers. *Phys. Rev. A: At., Mol., Opt. Phys.* **2014**, *90*, 050502.

(37) Ryabinkin, I. G.; Kohut, S. V.; Staroverov, V. N. Reduction of Electronic Wave Functions to Kohn-Sham Effective Potentials. *Phys. Rev. Lett.* **2015**, *115*, 083001.

(38) Wagner, L. O.; Stoudenmire, E.; Burke, K.; White, S. R. Guaranteed convergence of the kohn-sham equations. *Phys. Rev. Lett.* **2013**, *111*, 093003.

(39) Vuckovic, S.; Irons, T. J.; Savin, A.; Teale, A. M.; Gori-Giorgi, P. Exchange−correlation functionals via local interpolation along the adiabatic connection. *J. Chem. Theory Comput.* **2016**, *12*, 2598−2610.

(40) Becke, A. D. Density-functional exchange-energy approximation with correct asymptotic behavior. *Phys. Rev. A: At., Mol., Opt. Phys.* **1988**, *38*, 3098.

(41) Lee, C.; Yang, W.; Parr, R. G. Development of the Colle-Salvetti correlation-energy formula into a functional of the electron density. *Phys. Rev. B: Condens. Matter Mater. Phys.* **1988**, *37*, 785.

(42) Perdew, J. P.; Zunger, A. Self-interaction correction to density-functional approximations for many-electron systems. *Phys. Rev. B: Condens. Matter Mater. Phys.* **1981**, *23*, 5048.

(43) Perdew, J. P.; Burke, K.; Ernzerhof, M. Generalized Gradient Approximation Made Simple. *Phys. Rev. Lett.* **1996**, *77*, 3865.

(44) Perdew, J. P.; Ernzerhof, M.; Burke, K. Rationale for mixing exact exchange with density functional approximations. *J. Chem. Phys.* **1996**, *105*, 9982−9985.

(45) Perdew, J. P.; Schmidt, K. Jacob's ladder of density functional approximations for the exchange-correlation energy. *AIP Conference Proceedings.* **2000**, 1−20.

(46) Perdew, J. P. Climbing the ladder of density functional approximations. *MRS Bull.* **2013**, *38*, 743−750.

(47) Thomas, L. H. The calculation of atomic fields. *Math. Proc. Cambridge Philos. Soc.* **1927**, *23*, 542−548.

(48) Fermi, E. A statistical method for the determination of some priorieta dell'atome. *Rend. Accad. Nat. Lincei* **1927**, *6*, 32.

(49) Lieb, E. H.; Simon, B. The Thomas-Fermi theory of atoms, molecules and solids. *Advances in mathematics* **1977**, *23*, 22−116.

(50) Parr, R. G.; Yang, W. *Density-Functional Theory of Atoms and Molecules*; Oxford University Press: New York, 1989.

(51) Sun, Q.; Berkelbach, T. C.; Blunt, N. S.; Booth, G. H.; Guo, S.; Li, Z.; Liu, J.; McClain, J. D.; Sayfutyarova, E. R.; Sharma, S.; Wouters, S.; Chan, G. K.-L. PySCF: The Python-based simulations of chemistry framework. *Wiley Interdisciplinary Reviews: Computational Molecular Science* **2018**, *8*, e1340.

(52) Dunning, T. H. Gaussian basis sets for use in correlated molecular calculations. I. The atoms boron through neon and hydrogen. *J. Chem. Phys.* **1989**, *90*, 1007.

(53) Lieb, E. H.; Simon, B. Thomas-Fermi theory revisited. *Phys. Rev. Lett.* **1973**, *31*, 681.

(54) Burke, K.; Cancio, A.; Gould, T.; Pittalis, S. Locality of correlation in density functional theory. *J. Chem. Phys.* **2016**, *145*, 054112.

(55) Cancio, A.; Chen, G. P.; Krull, B. T.; Burke, K. Fitting a round peg into a round hole: Asymptotically correcting the generalized gradient approximation for correlation. *J. Chem. Phys.* **2018**, *149*, 084116.

(56) Lehtomäki, J.; Makkonen, I.; Caro, M. A.; Harju, A.; Lopez-Acevedo, O. Orbital-free density functional theory implementation with the projector augmented-wave method. *J. Chem. Phys.* **2014**, *141*, 234102.

(57) Constantin, L. A.; Fabiano, E.; Della Sala, F. Semilocal Pauli–Gaussian kinetic functionals for orbital-free density functional theory calculations of solids. *J. Phys. Chem. Lett.* **2018**, *9*, 4385−4390.

(58) Constantin, L. A.; Fabiano, E.; Della Sala, F. Performance of Semilocal Kinetic Energy Functionals for Orbital-Free Density Functional Theory. *J. Chem. Theory Comput.* **2019**, *15*, 3044−3055.

(59) Finzel, K. Local conditions for the Pauli potential in order to yield self-consistent electron densities exhibiting proper atomic shell structure. *J. Chem. Phys.* **2016**, *144*, 034108.

(60) March, N. The local potential determining the square root of the ground-state electron density of atoms and molecules from the Schrödinger equation. *Phys. Lett. A* **1986**, *113*, 476−478.

(61) Levy, M.; Ou-Yang, H. Exact properties of the Pauli potential for the square root of the electron density and the kinetic energy functional. *Phys. Rev. A: At., Mol., Opt. Phys.* **1988**, *38*, 625.

(62) Carrascal, D. J.; Ferrer, J.; Smith, J. C.; Burke, K. The Hubbard dimer: a density functional case study of a many-body problem. *J. Phys.: Condens. Matter* **2015**, *27*, 393001.

(63) Carrascal, D. J.; Ferrer, J.; Maitra, N.; Burke, K. Linear response time-dependent density functional theory of the Hubbard dimer. *Eur. Phys. J. B* **2018**, *91*, 142.

(64) Levy, M.; Görling, A. Correlation-energy density-functional formulas from correlating first-order density matrices. *Phys. Rev. A: At., Mol., Opt. Phys.* **1995**, *52*, R1808.